

Low-Complexity DoA Estimation using Transmissive Intelligent Surfaces

Jingyuan Zhang, Ching-Lun Tai, Raghupathy Sivakumar, and Douglas M. Blough

School of Electrical and Computer Engineering, Georgia Institute of Technology, Atlanta, GA, United States

Emails: {jingyuan_z, ctai32}@gatech.edu, {siva, doug.blough}@ece.gatech.edu

Abstract—A low-complexity direction of arrival (DoA) estimation approach based on transmissive intelligent surfaces (TISs) is proposed for single-target scenarios. The proposed DoA estimator is composed of one TIS with pre-designed phase shifts and two receive antennas. The signal from the target transmits through the TIS before being captured by the two antennas, and the DoA of the target is estimated solely based on the ratio of power received at the two antennas. An optimization method is proposed to design the phase shifts of the TIS and the relative positions of the two antennas with two primary objectives: (1) enhancing DoA estimation accuracy, and (2) guaranteeing an analytical expression of the estimated DoA derived from the power ratio. To be specific, the power ratio is approximated using a limited number of Fourier series coefficients, so that the optimization problem is formulated as a small set of quadratic programming problems aimed at optimizing these Fourier series coefficients. Simulation results validate the effectiveness of the proposed TIS-based DoA estimator and the optimization method. The method demonstrates comparable or even lower root mean squared error (RMSE) of DoA estimation in comparison to classic approaches. Unlike classic approaches that rely on complex-valued received signals, the proposed method offers reduced hardware complexity, relying solely on power measurements. Additionally, it involves reduced computational complexity compared to classic approaches including the multiple signal classification (MUSIC) algorithm and the discrete Fourier transform (DFT)-based DoA estimation method.

Index Terms—transmissive intelligent surfaces, direction of arrival, low-complexity, Fourier series, quadratic programming

I. INTRODUCTION

Reconfigurable intelligent surfaces (RISs) [1] have gained increasing popularity in the field of wireless communications due to their capability of shaping the propagation path of incident electromagnetic (EM) waves. With flexible configuration of the phase shift of each RIS element, RISs create a favorable propagation environment for wireless networks, whose spectrum and energy efficiency can be significantly enhanced [2].

As a particular type of RIS, transmissive intelligent surfaces (TISs) [3] are an emerging and promising option. TISs transmit any incident EM wave through and can alter its propagation direction, leading to a broad coverage in wireless networks. Several previous works have explored the feasibility of accommodating TISs for the purpose of coverage expansion. In [4], the authors propose a conceptual RIS design which incorporates TISs, developing three realistic protocols: energy splitting, mode switching, and time switching. The authors of [5] implement a millimeter-wave (mmWave) RIS structure

with TISs included, which can be integrated into common mmWave link discovery protocols.

With their ability to steer incident EM waves and generate beams of desired directions, TISs can be leveraged to conduct target detection, such as direction of arrival (DoA) estimation of a target. For DoA estimation, numerous methods based on the classic multiple signal classification (MUSIC) algorithm [6] have been proposed (e.g., [7], [8]). However, these methods suffer from a large post-processing overhead caused by signal decoding and demodulation with a need of phase difference computation. In addition, there is some prior research focused on TIS-specific DoA estimation methods (e.g., [9]–[11]). As these methods require a frequent phase shift reconfiguration of TISs, they are limited by a high hardware complexity. Overall, the DoA estimation methods discussed above are not suitable for edge devices with limited computation resources.

In this paper, we propose a novel low-complexity TIS-based DoA estimator targeting at edge devices. Specifically, the proposed method employs the power ratio from two receive antennas for DoA estimation with a TIS under fixed phase shifts, resulting in a small post-processing overhead and a low hardware complexity. To determine the location of two receive antennas and the fixed phase shifts of the TIS, we formulate a corresponding optimization problem, which is transformed into a small set of more tractable quadratic optimization problems by approximating the power ratio using a finite number of Fourier series. Furthermore, an analytical expression of the estimated DoA derived from the power ratio is guaranteed by using the proposed optimization method.

The remainder of this paper is organized as follows. Sec. II introduces the system model and problem formulation of the TIS-based DoA estimator. Sec. III discusses the proposed optimization approach for optimizing the TIS-based DoA estimator and the method to estimate DoA from measured power ratio. Sec. IV demonstrates simulation results of DoA estimation performance using the proposed method. Finally, Sec. V concludes the paper.

II. SYSTEM MODEL AND PROBLEM FORMULATION

A. System Model

The system model of single-target DoA detection is illustrated in Fig. 1. The proposed DoA estimator is composed of a TIS and two receive antennas, and the distances between the two antennas to the center of the TIS array are the same. Moreover, it is assumed that both the target and the receive

antennas are in the far field region of the TIS. The TIS features two columns of elements, where there are N TIS elements in each column sharing an identical transmission coefficient and the spacing between two adjacent TIS elements is d . Moreover, let $\gamma_{i_c} = e^{j\varphi_{i_c}}$ denote the transmission coefficient of elements in the i_c^{th} column, where φ_{i_c} is the corresponding phase shift and $i_c \in \{1, 2\}$. Let $\theta_k \in (-\frac{\pi}{2}, \frac{\pi}{2})$ represent the direction of the k^{th} antenna, where $k \in \{1, 2\}$ and $\theta_1 = -\theta_2$. Although the proposed TIS-based DoA estimator can work at various frequency bands, we focus on mmWave band in this paper as TIS arrays at mmWave band can be small which are suitable for edge devices.

It is assumed that the target actively transmits signals with power P_t . Given the direction of the target as $\theta \in [-\frac{\pi}{2}, \frac{\pi}{2}]$, the signal received from the line-of-sight (LoS) path at the k^{th} antenna is

$$y_k(\theta) = \sqrt{P_t g_k} N x \sum_{i_c=1}^2 e^{j\varphi_{i_c}} e^{-j\frac{2\pi}{\lambda}(i_c-1)d(\sin(\theta)+\sin(\theta_k))}, \quad (1)$$

where λ is the wavelength, x is the symbol transmitted from the target such that $\mathbb{E}(\|x\|_2^2) = 1$, and g_k is the cascaded channel gain from the target to the TIS and from the TIS to the k^{th} receive antenna. Then the power received at the k^{th} antenna is given by

$$P_k(\theta) = 2P_t g_k N^2 \left(1 + \cos(z \sin(\theta) + z \sin(\theta_k) + \Delta\varphi)\right), \quad (2)$$

where $z = \frac{2\pi}{\lambda}d$ and $\Delta\varphi = \varphi_1 - \varphi_2$. Moreover, we have $g_1 = g_2$ since the distances between the two antennas to the center of the TIS are the same. Then the ratio of the power received at the two antennas is

$$\alpha(\theta) = \frac{P_1(\theta)}{P_2(\theta)} = \frac{1 + \cos(z \sin(\theta) + f(\theta_1, \Delta\varphi))}{1 + \cos(z \sin(\theta) + f(\theta_2, \Delta\varphi))}, \quad (3)$$

where

$$f(\theta_k, \Delta\varphi) = z \sin(\theta_k) + \Delta\varphi. \quad (4)$$

B. Problem Formulation

In this paper, the goal is to design the parameters of the TIS-based DoA estimator, which are $\Delta\varphi$ and θ_1 , in order to estimate the DoA of the target only from the power ratio $\alpha(\theta)$. Therefore, $\alpha(\theta) : \theta \rightarrow \alpha$ should be a bijective function when $\theta \in [-\frac{\pi}{2}, \frac{\pi}{2}]$. For practicality in real-world implementation, $\alpha(\theta)$ can be designed as an either monotonically increasing or decreasing function for $\theta \in [-\frac{\pi}{2}, \frac{\pi}{2}]$. Without loss of generality, we opt for $\alpha(\theta)$ to monotonically increase within this range. Additionally, to improve distinguishability among different θ values, the gradient $\frac{\partial\alpha}{\partial\theta}$ should be maximized. Hence, the problem of optimizing parameters of the TIS-based DoA estimator can be formulated as

$$\max_{\Delta\varphi, \theta_1} \mathbb{E}_{\theta \in [-\frac{\pi}{2}, \frac{\pi}{2}]} \left(\frac{\partial\alpha}{\partial\theta} \right) \quad (5a)$$

$$\text{s.t.} \quad \frac{\partial\alpha}{\partial\theta} \geq 0, \forall \theta \in [-\frac{\pi}{2}, \frac{\pi}{2}]. \quad (5b)$$

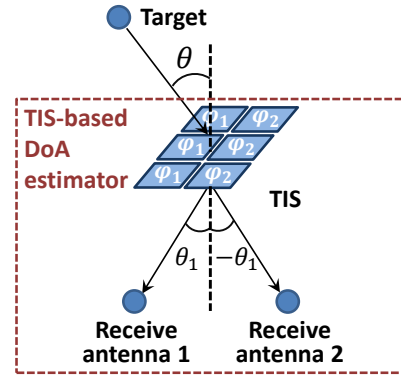


Fig. 1. Illustration of the proposed TIS-based DoA estimator.

Furthermore, the optimization should ensure an analytical expression of θ derived from the power ratio $\alpha(\theta)$. After the DoA estimation device parameters are designed, the phase shifts φ_1 and φ_2 for TIS elements remain constant during the DoA detection stage, which simplifies hardware complexity compared to reconfigurable TISs.

III. OPTIMIZATION OF TIS-BASED DOA ESTIMATOR

In this section, the optimization problem (5) is transformed into a set of quadratic programming problems by utilizing Fourier series, with the aim to improve DoA estimation accuracy and ensure an analytical expression of estimated θ from power ratio $\alpha(\theta)$. The design of parameters of the proposed TIS-based DoA estimator is introduced first. Then the method of estimating the target direction θ from the power ratio $\alpha(\theta)$ is presented.

A. Design of TIS-based DoA Estimator

In this subsection, the transformation of the original optimization problem into a set of quadratic programming problems is introduced. The key idea is to utilize a finite number of Fourier series coefficients to approximate the term $\alpha(\theta)$. Then the original problem is transformed into optimizing these Fourier series coefficients.

1) Expressing $\alpha(\theta)$ using Fourier series:

The term $1 + \cos(z \sin(\theta) + f(\theta_k, \Delta\varphi))$ can be expressed using Fourier series in sine-cosine form as

$$\begin{aligned} & 1 + \cos(z \sin(\theta) + f(\theta_k, \Delta\varphi)) \\ &= 1 + \cos(z \sin(\theta)) \cos(f(\theta_k, \Delta\varphi)) - \sin(z \sin(\theta)) \sin(f(\theta_k, \Delta\varphi)) \\ &\stackrel{(a)}{=} 1 + \cos(f(\theta_k, \Delta\varphi)) \left(J_0(z) + 2 \sum_{n=1}^{\infty} J_{2n}(z) \cos(2n\theta) \right) \\ &\quad - \sin(f(\theta_k, \Delta\varphi)) \left(2 \sum_{n=1}^{\infty} J_{2n-1}(z) \sin((2n-1)\theta) \right), \end{aligned} \quad (6)$$

where (a) comes from Jacobi–Anger expansion [12], and $J_n(z)$ is the n^{th} Bessel function of the first kind.

Therefore, $1 + \cos(z \sin(\theta) + f(\theta_k, \Delta\varphi))$ can be expressed by Fourier series in exponential form, such that

$$1 + \cos(z \sin(\theta) + f(\theta_k, \Delta\varphi)) = \sum_{n=-\infty}^{\infty} C_{k,n} e^{jn\theta}, \quad (7)$$

where $C_{k,n}$ is the coefficient of Fourier series in exponential form and is given by

$$C_{k,n} = \begin{cases} a_{k,0}, & \text{if } n = 0, \\ \frac{1}{2}(a_{k,n} - jb_{k,n}), & \text{if } n > 0, \\ \frac{1}{2}(a_{k,|n|} + jb_{k,|n|}), & \text{if } n < 0, \end{cases} \quad (8)$$

where

$$a_{k,n} = \begin{cases} 1 + \cos(f(\theta_k, \Delta\varphi))J_0(z), & \text{if } n = 0, \\ 0, & \text{if } n > 0 \text{ and } n \text{ is odd,} \\ 2 \cos(f(\theta_k, \Delta\varphi))J_n(z), & \text{if } n > 0 \text{ and } n \text{ is even,} \end{cases} \quad (9)$$

$$b_{k,n} = \begin{cases} 0, & \text{if } n \geq 0 \text{ and } n \text{ is even,} \\ -2 \sin(f(\theta_k, \Delta\varphi))J_n(z), & \text{if } n > 0 \text{ and } n \text{ is odd.} \end{cases} \quad (10)$$

Furthermore, given the nature of DoA detection, $\alpha(\theta)$ should show periodicity with respect to θ , with a period of 2π . Thus, $\alpha(\theta)$ can be represented using Fourier series in sine-cosine form as

$$\alpha(\theta) = a_{3,0} + \sum_{n=1}^{\infty} (a_{3,n} \cos(n\theta) + b_{3,n} \sin(n\theta)), \quad (11)$$

where $a_{3,n}$ and $b_{3,n}$ are the Fourier series coefficients. Then the corresponding coefficient of Fourier series in exponential form is denoted by $C_{3,n}$. Let $\mathbf{C}_m = [C_{m,-\infty}, \dots, C_{m,-1}, C_{m,0}, C_{m,1}, \dots, C_{m,\infty}]$ be the vector containing all the coefficients $C_{m,n}$ of Fourier series in exponential form given m , where $m \in \{1, 2, 3\}$.

In summary, \mathbf{C}_1 , \mathbf{C}_2 , and \mathbf{C}_3 represent vectors containing coefficients of Fourier series in exponential form for $1 + \cos(z \sin(\theta) + f(\theta_1, \Delta\varphi))$, $1 + \cos(z \sin(\theta) + f(\theta_2, \Delta\varphi))$, and $\alpha(\theta)$, respectively. Then given the convolution theorems of Fourier series and (3), we have

$$\mathbf{C}_3 * \mathbf{C}_2 = \mathbf{C}_1. \quad (12)$$

For tractability, \mathbf{C}_1 , \mathbf{C}_2 , and \mathbf{C}_3 will be truncated into vectors with finite lengths, denoted by $\hat{\mathbf{C}}_1$, $\hat{\mathbf{C}}_2$, and $\hat{\mathbf{C}}_3$, which will be introduced next.

2) **Approximating $\alpha(\theta)$ using a small number of Fourier series coefficients:**

- Truncating \mathbf{C}_1 and \mathbf{C}_2 :

RIS element spacing is typically from $\frac{\lambda}{8}$ to $\frac{\lambda}{2}$ [13]. Therefore, given the possible value of z , the value of $|J_n(z)|$ approaches 0 as $|n| \rightarrow \infty$, which indicates that a limited number of $C_{k,n}$ where $k \in \{1, 2\}$ can be used to approximate $1 + \cos(z \sin(\theta) + f(\theta_1, \Delta\varphi))$ and $1 + \cos(z \sin(\theta) + f(\theta_2, \Delta\varphi))$. Considering possible values of z , coefficients $C_{k,n}$ for $n \in \{-6, -5, \dots, -1, 0, 1, \dots, 5, 6\}$ are selected, since $\frac{\sum_{n=-6}^6 J_n(z)}{\sum_{n=-\infty}^{\infty} J_n(z)} > 0.998$ which indicates that most of the information in $C_{k,n}$ is kept.

- Truncating \mathbf{C}_3 :

For the Fourier series vector \mathbf{C}_3 , only the Fourier series coefficients $C_{3,n}$ with $n \in \{-3, -2, -1, 0, 1, 2, 3\}$ are selected to approximate $\alpha(\theta)$. There are two reasons to support this choice: (1) The number of coefficients selected for $C_{1,n}$ and $C_{2,n}$ is the same as discussed above, which reduces the required number of coefficients in \mathbf{C}_3 in order to approximate $\mathbf{C}_3 * \mathbf{C}_2 = \mathbf{C}_1$. (2) An analytical inverse function from $\alpha(\theta)$ to θ is required for DoA estimation. However, if $C_{3,n}$ where $|n| > 3$ is maintained, the analytical function will become complicated or may not exist.

Furthermore, to guarantee the existence of an analytical inverse function from $\alpha(\theta)$ to θ , we set $a_{3,1} = b_{3,2} = a_{3,3} = 0$. In this case, we have

$$\begin{aligned} \alpha(\theta) &= a_{3,0} + b_{3,1} \sin(\theta) + a_{3,2} \cos(2\theta) + b_{3,3} \sin(3\theta) \\ &= -4b_{3,3} \sin^3(\theta) - 2a_{3,2} \sin^2(\theta) \\ &\quad + (b_{3,1} + 3b_{3,3}) \sin(\theta) + a_{3,2} + a_{3,0}, \end{aligned} \quad (13)$$

which is a cubic equation with respect to $\sin(\theta)$, and can be used to get the inverse function from $\alpha(\theta)$ to θ as will be discussed in Sec. III-B.

In other words, the condition of $\mathbf{C}_3 * \mathbf{C}_2 = \mathbf{C}_1$ can be turned into

$$\hat{\mathbf{C}}_3 * \hat{\mathbf{C}}_2 \approx \hat{\mathbf{C}}_1, \quad (14)$$

where

$$\hat{\mathbf{C}}_1 = [0, 0, 0, C_{1,-6}, C_{1,-5}, \dots, C_{1,0}, \dots, C_{1,5}, C_{1,6}, 0, 0, 0], \quad (15)$$

$$\hat{\mathbf{C}}_2 = [C_{2,-6}, C_{2,-5}, \dots, C_{2,0}, \dots, C_{2,5}, C_{2,6}], \quad (16)$$

$$\hat{\mathbf{C}}_3 = [j \frac{b_{3,3}}{2}, \frac{a_{3,2}}{2}, j \frac{b_{3,1}}{2}, a_{3,0}, -j \frac{b_{3,1}}{2}, \frac{a_{3,2}}{2}, -j \frac{b_{3,3}}{2}]. \quad (17)$$

3) **Transforming the TIS-based DoA estimator optimization problem into a set of quadratic programming problems:**

Since $\frac{\partial \alpha}{\partial \theta} = b_{3,1} \cos(\theta) - 2a_{3,2} \sin(2\theta) + 3b_{3,3} \cos(3\theta)$ with approximation discussed in Sec. III-A2, the objective function in (5a) can be interpreted as $\mathbb{E}_{\theta \in [-\frac{\pi}{2}, \frac{\pi}{2}]} \left(\frac{\partial \alpha}{\partial \theta} \right) = 2b_{3,1} - 2b_{3,3}$.

Moreover, since $\frac{\partial \alpha}{\partial \theta} = \cos(\theta)(b_{3,1} - 4a_{3,2} \sin(\theta) + 3b_{3,3}(1 - 4 \sin^2(\theta)))$, the constraint of $\frac{\partial \alpha}{\partial \theta} \geq 0$ for $\theta \in [-\frac{\pi}{2}, \frac{\pi}{2}]$ can be interpreted as $b_{3,1} - 4a_{3,2} \sin(\theta) + 3b_{3,3}(1 - 4 \sin^2(\theta)) \geq 0$ for $\theta \in [-\frac{\pi}{2}, \frac{\pi}{2}]$.

In other words, the optimization problem (5) can be transformed into

$$\max_{\Delta\varphi, \theta_1} 2b_{3,1} - 2b_{3,3} \quad (18a)$$

$$\text{s.t. } \|\hat{\mathbf{C}}_3 * \hat{\mathbf{C}}_2 - \hat{\mathbf{C}}_1\|_{\infty} \leq \epsilon, \quad (18b)$$

$$\text{if } b_{3,3} \geq 0 \text{ or } \{b_{3,3} < 0 \text{ and } \frac{a_{3,2}}{6b_{3,3}} \geq 1\} \text{ or}$$

$$\{b_{3,3} < 0 \text{ and } \frac{a_{3,2}}{6b_{3,3}} \leq -1\}, \text{ then}$$

$$b_{3,1} - 9b_{3,3} \geq |4a_{3,2}|, \quad (18c)$$

$$\text{if } b_{3,3} < 0 \text{ and } \left| \frac{a_{3,2}}{6b_{3,3}} \right| < 1, \text{ then}$$

$$b_{3,1} + 4a_{3,2} \left(\frac{a_{3,2}}{6b_{3,3}} \right) + 3b_{3,3} (1 - 4 \left(\frac{a_{3,2}}{6b_{3,3}} \right)^2) \geq 0, \quad (18d)$$

where ϵ is a small positive value, and constraints (18c) and (18d) are used to ensure that $\frac{\partial \alpha}{\partial \theta} \geq 0$ for $\theta \in [-\frac{\pi}{2}, \frac{\pi}{2}]$. In this case, the parameters of the proposed TIS-based DoA estimator can be optimized, and meanwhile an analytical expression from power ratio $\alpha(\theta)$ to estimated DoA θ can be ensured.

Furthermore, the optimization problem (18) can be turned into finding the solutions of four quadratic programming problems with the same objective function (18a). The optimal solution that can offer the minimal value of the objective function will be selected from these four solutions. The l^{th} quadratic programming problem where $l \in \{0, 1, 2, 3\}$ is defined as

$$\min_{\mathbf{x}} \mathbf{f}_o^\top \mathbf{x} \quad (19a)$$

$$\text{s.t. } \mathbf{x}^\top \mathbf{H}_s \mathbf{x} + \mathbf{w}_s^\top \mathbf{x} + r_s \leq 0, \text{ for } s \in \{0, 1, \dots, 19\}, \quad (19b)$$

$$\mathbf{x}^\top \mathbf{J}_{l,u} \mathbf{x} + \mathbf{p}_{l,u}^\top \mathbf{x} \leq 0, \quad (19c)$$

$$\text{for } u \in \{0, 1, 2\} \text{ when } l = 0,$$

$$\text{and } u \in \{0, 1, 2, 3\} \text{ when } l \in \{1, 2, 3\},$$

$$\mathbf{x}^\top \mathbf{G}_v \mathbf{x} + c_v = 0, \text{ for } v \in \{0, 1\}, \quad (19d)$$

where $\mathbf{f}_o, \mathbf{w}_s, \mathbf{p}_{l,u} \in \mathbb{R}^{8 \times 1}$, $\mathbf{H}_s, \mathbf{J}_{l,u}, \mathbf{G}_v \in \mathbb{R}^{8 \times 8}$, and $r_s, c_v \in \mathbb{R}$ are given in Appendix, and $\mathbf{x} \in \mathbb{R}^{8 \times 1}$ is determined as

$$\mathbf{x} = [a_{3,0}, b_{3,1}, a_{3,2}, b_{3,3}, \cos(f(\theta_1, \Delta\varphi)), \sin(f(\theta_1, \Delta\varphi)), \cos(f(-\theta_1, \Delta\varphi)), \sin(f(-\theta_1, \Delta\varphi))]^\top. \quad (20)$$

Herein, constraint (19b) ensures that constraint (18b) is satisfied, and constraint (19c) in the four quadratic programming problems ensures that constraints (18c) and (18d) are satisfied. Moreover, constraint (19d) is used to guarantee that $\cos^2(f(\theta_k, \Delta\varphi)) + \sin^2(f(\theta_k, \Delta\varphi)) = 1$ where $k \in \{1, 2\}$.

Let $[\mathbf{x}]_n$ denote the n^{th} entry in vector \mathbf{x} , where $n \in \{0, 1, \dots, 7\}$. Then the overall algorithm for designing parameters of the proposed TIS-based DoA estimator is given in Algorithm 1.

B. Estimation of DoA Based on Power Ratio

After the parameters of TIS-based DoA estimator are designed using Algorithm 1, the function $\alpha(\theta) = a_{3,0} + b_{3,1} \sin(\theta) + a_{3,2} \cos(2\theta) + b_{3,3} \sin(3\theta)$ for $\theta \in [-\frac{\pi}{2}, \frac{\pi}{2}]$ is determined. Then the analytical result of the estimated DoA $\tilde{\theta}$ can be acquired from measured power ratio $\tilde{\alpha}$, as the value of $\sin(\tilde{\theta})$ can be obtained by solving the cubic equation (13). The method for DoA estimation based on power ratio is given in Algorithm 2.

C. Received Power Enhancement

The accuracy of DoA estimation depends on the signal-to-noise ratio (SNR) at the receive antennas. One approach to improve SNR is to enhance the received power at the antennas by expanding TIS dimension N . However, given a fixed distance between TIS and two receive antennas, increasing N may result in the two antennas not being located in the far-field region of the entire TIS array. To mitigate the near-field

Algorithm 1: System design of the proposed TIS-based DoA estimator

Input: Wavelength λ , TIS element spacing d , error bound ϵ

Output: Receive antenna direction θ_1 , TIS phase shift difference $\Delta\varphi$, $a_{3,0}$, $b_{3,1}$, $a_{3,2}$, $b_{3,3}$

Solve the l^{th} quadratic programming problem defined in (19) to get solution \mathbf{x}_l where $l \in \{0, 1, 2, 3\}$

Get $\mathbf{x} = \arg \min_{\mathbf{x}_l} \mathbf{f}_o^\top \mathbf{x}_l$

$a_{3,0} \leftarrow [\mathbf{x}]_0$

$b_{3,1} \leftarrow [\mathbf{x}]_1$

$a_{3,2} \leftarrow [\mathbf{x}]_2$

$b_{3,3} \leftarrow [\mathbf{x}]_3$

Get $f_1 \in [-\pi, \pi]$ from $\cos(f_1) = [\mathbf{x}]_4$ and

$\sin(f_1) = [\mathbf{x}]_5$, where f_1 denotes $f(\theta_1, \Delta\varphi)$ in (4)

Get $f_2 \in [-\pi, \pi]$ from $\cos(f_2) = [\mathbf{x}]_6$ and

$\sin(f_2) = [\mathbf{x}]_7$, where f_2 denotes $f(\theta_2, \Delta\varphi)$ in (4)

$\theta_1 \leftarrow \arcsin\left(\frac{(f_1 - f_2)\lambda}{4\pi d}\right)$

$\Delta\varphi \leftarrow f_1 - \frac{2\pi d}{\lambda} \sin(\theta_1)$

Algorithm 2: DoA estimation based on power ratio

Input: $a_{3,0}$, $b_{3,1}$, $a_{3,2}$, $b_{3,3}$, and the ratio of power received at two antennas $\tilde{\alpha}$

Output: Estimated DoA ($\tilde{\theta}$) of the target

$\tilde{\alpha} \leftarrow \min(\tilde{\alpha}, \alpha(\frac{\pi}{2}))$

$\tilde{\alpha} \leftarrow \max(\tilde{\alpha}, \alpha(-\frac{\pi}{2}))$

Solve

$$4b_{3,3}x^3 + 2a_{3,2}x^2 - (b_{3,1} + 3b_{3,3})x - a_{3,0} - a_{3,2} + \tilde{\alpha} = 0,$$

and get the real root x which satisfies $x \in [-1, 1]$

$\tilde{\theta} = \arcsin(x)$

effects, an additional phase shift $\Delta\varphi_{i_c, i_r}$ is introduced to the $(i_c, i_r)^{\text{th}}$ TIS element located at the i_c^{th} column and the i_r^{th} row, where $i_c \in \{1, 2\}$ and $i_r \in \{1, 2, \dots, N\}$. This phase shift is given by $\Delta\varphi_{i_c, i_r} = \frac{2\pi}{\lambda} d_{i_c, i_r}$, where d_{i_c, i_r} is the distance between the i_c^{th} receive antenna and the $(i_c, i_r)^{\text{th}}$ TIS element. Therefore, the overall phase shift of the $(i_c, i_r)^{\text{th}}$ TIS element is $\hat{\varphi}_{i_c, i_r} = \varphi_{i_c} + \Delta\varphi_{i_c, i_r}$.

IV. SIMULATION

A. Simulation Settings

An indoor office model from MATLAB [14], which is illustrated in Fig. 2, is used to generate the mmWave ray tracing channel between the target and the TIS. The length, width, and height of the room are 8 m, 5 m, and 3 m, respectively. The distance between the target and the TIS-based DoA estimator is set as 1.5 m, and the distance between the two receive antennas to the center of TIS is 0.05 m. The maximum transmit power of the target and the noise power are set as 24 dBm and -100 dBm, respectively. The operating frequency is set as 28 GHz. The TIS-based DoA estimator is assumed to be randomly located in the room. Since the proposed method is designed for the scenario where the LoS

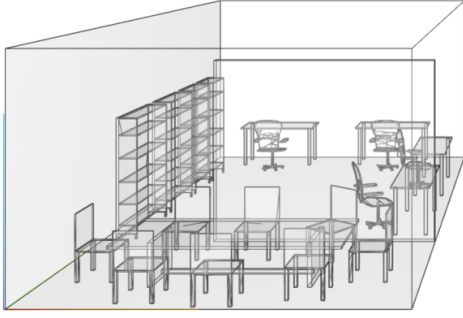


Fig. 2. An illustration of the indoor simulation scenario.

path between the target and the TIS exists, those random locations where the LoS path does not exist are discarded.

B. Designing Parameters of the Proposed TIS-Based DoA Estimator

To validate the proposed method, Algorithm 1 is used to design θ_1 and $\Delta\varphi$ used for the proposed TIS-based DoA estimator, and $a_{3,0}$, $b_{3,1}$, $a_{3,2}$, and $b_{3,3}$ used during the DoA detection stage. Three values of TIS element spacing, d , are considered: $\frac{\lambda}{4}$, $\frac{\lambda}{6}$, and $\frac{\lambda}{8}$. Note that the error bound ϵ will influence the design of system parameters. A large ϵ may yield inaccuracies in approximating the function $\alpha(\theta)$, whereas an excessively small ϵ could result in the absence of feasible solutions. Herein, ϵ is set to 0.0005, 0.0001, and 0.0001 for $d = \frac{\lambda}{4}$, $d = \frac{\lambda}{6}$, and $d = \frac{\lambda}{8}$, respectively.

The designed parameters are listed in Table. I. Given the designed θ_1 and $\Delta\varphi$, the theoretical power ratio function $\alpha(\theta)$ in Eq. (3) and the approximated function as in Eq. (13) are shown in Fig. 3. According to Fig. 3, there is only a slight gap between the theoretical and the approximated power ratio function $\alpha(\theta)$, which validates the proposed approximation method based on a limited number of Fourier series coefficients.

Given the designed parameters, the root mean squared error (RMSE) of DoA estimation using Algorithm 2 is shown in Fig. 4. Two scenarios are tested: (1) only the LoS path between the target and the TIS is considered, and (2) the LoS path and reflection paths between the target and the TIS are considered. Case (1) represents an ideal case, which is used to verify the proposed DoA estimation method based on the approximated $\alpha(\theta)$. Case (2) represents a more realistic case, which provides insights into performance of the proposed method in a real-world setting. Herein, the TIS size is set as 2×8 . According to Fig. 4, TIS with $d = \frac{\lambda}{4}$ generally shows the lowest RMSE in both Case (1) and Case (2), while TIS with $d = \frac{\lambda}{8}$ generally demonstrates the highest RMSE. This is because the power ratio function $\alpha(\theta)$ for TIS with $d = \frac{\lambda}{4}$ shows the highest value of $\mathbb{E}_{\theta \in [-\frac{\pi}{2}, \frac{\pi}{2}]} \left(\frac{\partial \alpha}{\partial \theta} \right)$ according to Fig. 3, indicating better distinguishability among different DoAs. In both Case (1) and Case (2), the RMSE is greater when $|\theta|$ approaches $\frac{\pi}{3}$ compared to when $\theta = 0$. This is also due to the higher value of $|\frac{\partial \alpha}{\partial \theta}|$ near $\theta = 0$ compared to $|\theta| = \frac{\pi}{3}$. In Case (1), the RMSE for TIS with $d = \frac{\lambda}{4}$ remains below 2° , whereas it rises to the range of $[7, 23]^\circ$ in Case (2) due to multipath effects.

TABLE I
DESIGNED DOA ESTIMATION DEVICE PARAMATERS

d	θ_1 (rad)	$\Delta\varphi$ (rad)	$a_{3,0}$	$b_{3,1}$	$a_{3,2}$	$b_{3,3}$
$\frac{\lambda}{4}$	-0.2182	-0.9737	0.6732	0.5570	0.0214	-0.0257
$\frac{\lambda}{6}$	-0.3471	-1.3338	0.5433	0.3730	0.0219	-0.0068
$\frac{\lambda}{8}$	-0.4011	-1.7501	0.4451	0.3017	0.0277	-0.0039

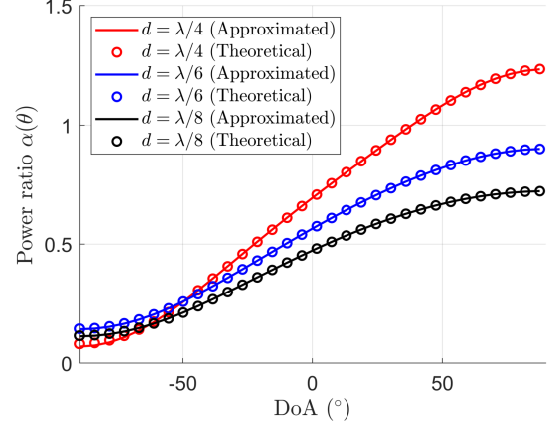


Fig. 3. Designed function $\alpha(\theta)$ for different TIS element spacings.

C. Comparison with Classic DoA Estimation Methods

To further evaluate the proposed method, a comparison is conducted among the proposed method and classic DoA estimation methods. The case of TIS with $d = \frac{\lambda}{4}$ is chosen for the proposed method, as it demonstrates the best performance among the three TIS spacing values considered. Moreover, the TIS size is set as 2×8 . For the classic methods, three approaches are selected: the MUSIC algorithm [6], phase-difference-of-arrival (PDOA) algorithm [15], and a discrete Fourier transform (DFT)-based DoA estimation method [16]. Given that the proposed method employs two antennas, it is assumed that the three classic approaches also utilize only two antennas for the purpose of a fair comparison. For classic approaches, the distance between the two antennas is set at $\frac{\lambda}{2}$,

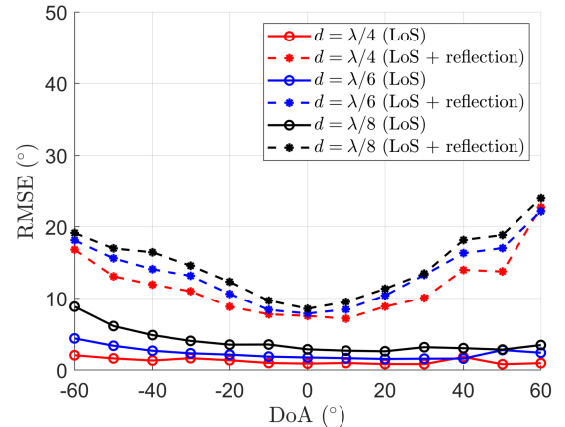


Fig. 4. RMSE of DoA estimation with different TIS element spacings (TIS size 2×8).

with their center positioned at the same location as the center of the TIS in the proposed method.

Fig. 5 illustrates the DoA estimation performance of both the proposed method and classic approaches in scenarios where both the LoS path and reflection paths are taken into account. It can be observed that the three classic approaches exhibit similar performances. Particularly, within the range of $\theta \in [-\frac{\lambda}{6}, \frac{\lambda}{6}]$, the RMSE of the proposed method closely aligns with that of the classic approaches. However, as $|\theta|$ gets close to $\frac{\lambda}{3}$, the RMSE of classic approaches reaches approximately 45° , while the RMSE of the proposed method remains below 25° .

The results demonstrate the advantages of the proposed method in that it shows comparable or even superior performance to classic approaches, alongside lower hardware or computation complexity. The proposed method only relies on power measurement, while all the three classic approaches require complex-valued received signals for DoA estimation, thereby increasing hardware complexity for signal detection. Furthermore, MUSIC algorithm and DFT-based DoA estimation have higher computation complexity than PDOA and the proposed method. The MUSIC algorithm requires singular value decomposition (SVD) of the correlation matrix of the received signal across antennas, and calculation of the pseudo-spectrum using a series of steering vectors where the DoA is estimated by searching for the peak in the pseudo-spectrum. In addition to the computational complexity associated with SVD, the complexity increases when a higher resolution of the pseudo-spectrum is required. Given that two antennas are used in the simulation, the computational complexity for calculating the pseudo-spectrum is $O(N_m)$, where N_m is the number of steering vectors. The resolution of DoA estimation in the DFT-based method depends on the number of DFT points, represented by N_d , with the computational complexity of DFT being $O(N_d^2)$. Compared to the MUSIC algorithm and the DFT-based method, both PDOA and the proposed method have constant computational complexity. Although the proposed method entails calculating roots of a cubic equation, resulting in a slightly higher computational complexity than PDOA, it demonstrates lower hardware complexity and shows lower RMSE when $|\theta|$ increases, as illustrated in Fig. 5.

D. Received Power Enhancement

The performance of the received power enhancement strategy described in Sec. III-C is evaluated. The TIS element spacing is selected as $d = \frac{\lambda}{4}$, and three TIS sizes are chosen: 2×4 , 2×8 , and 2×16 . Fig. 6 shows the RMSE of DoA estimation when the ground truth is $\theta = \frac{\pi}{6}$. According to Fig. 6, the TIS with size 2×16 shows the lowest RMSE, while the TIS with size 2×4 has the highest RMSE, given a specific transmit power. To achieve an RMSE below 15° , the minimum transmit power for TIS with sizes of 2×16 , 2×8 , and 2×4 is approximately 1 dBm, 7 dBm, and 12.5 dBm, respectively. This observation validates the effectiveness of the proposed received power enhancement strategy.

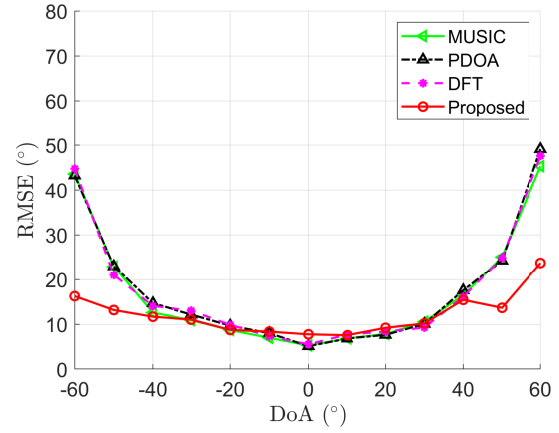


Fig. 5. RMSE of DoA estimation for different methods (two receive antennas for each method, TIS size 2×8).

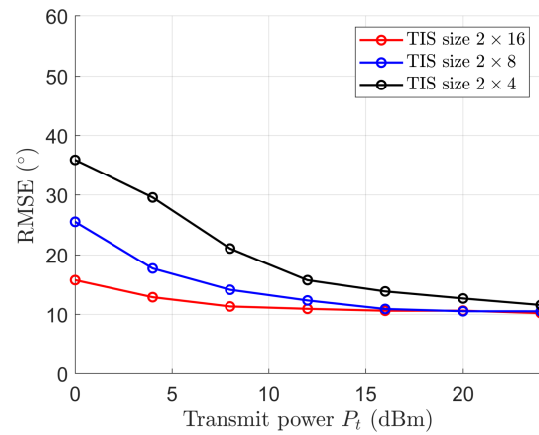


Fig. 6. RMSE of DoA estimation for different TIS sizes (TIS element spacing $d = \frac{\lambda}{4}$, ground truth DoA $\theta = \frac{\pi}{6}$).

V. CONCLUSION

A low-complexity TIS-based DoA estimator is introduced for single-target scenarios. The design of the system parameters is formulated as a set of quadratic programming problems, allowing for the analytical estimation of DoA using the proposed method. This estimator offers the advantage of reduced hardware complexity, as it only requires power measurement. Additionally, it has reduced computational complexity compared to classic DoA estimation methods such as the MUSIC algorithm and DFT-based approach.

ACKNOWLEDGMENT

This work was supported in part by the Wayne J. Holman Chair and the EVP for Research at Georgia Tech.

APPENDIX

Let $\mathbf{e}_i \in \mathbb{R}^{8 \times 1}$ represent a vector where all entries are zero except for the i^{th} entry, which is set to 1, where $i \in \{0, 1, \dots, 7\}$. Furthermore, let $\mathbf{E}_{i,j} \in \mathbb{R}^{8 \times 8}$ be a matrix with all entries being zero except for the $(i, j)^{\text{th}}$ and $(j, i)^{\text{th}}$

entries, both of which are set to 1, where $i, j \in \{0, 1, \dots, 7\}$. Then \mathbf{f}_o used in the objective function (19a) is given by

$$\mathbf{f}_o = -2\mathbf{e}_1 + 2\mathbf{e}_3. \quad (21)$$

\mathbf{H}_s , \mathbf{w}_s , and r_s for $s \in \{0, 1, \dots, 19\}$ used in constraint (19b) are given by

$$\mathbf{H}_s = \begin{cases} \frac{J_{6-s}(z) - J_{12-s}(z)U(s-6)}{4} \mathbf{E}_{3,6+\text{mod}(s,2)} \\ + \frac{J_{s-7}(z)U(s-1) + J_{s-11}(z)U(s-5)}{4} \mathbf{E}_{2,6+\text{mod}(s+1,2)} \\ + \frac{J_{s-8}(z)U(s-2) - J_{10-s}(z)U(s-4)}{4} \mathbf{E}_{1,6+\text{mod}(s,2)} \\ + \frac{J_{s-9}(z)U(s-3)}{2} \mathbf{E}_{0,6+\text{mod}(s+1,2)}, \\ \quad \text{if } s \in \{0, 1, \dots, 9\}, \\ -\mathbf{H}_{s-10}, \text{ if } s \in \{10, 11, \dots, 19\}, \end{cases} \quad (22)$$

$$\mathbf{w}_s = \begin{cases} \mathbf{0}, & \text{if } s \in \{0, 1, 2\}, \\ \frac{1}{2}(\lfloor \frac{s}{3} \rfloor - 1)\mathbf{e}_{9-s} + (-1)^s J_{9-s}(z)\mathbf{e}_{5-\text{mod}(s,2)}, \\ \quad \text{if } s \in \{3, 4, \dots, 9\}, \\ -\mathbf{w}_{s-10}, & \text{if } s \in \{10, 11, \dots, 19\}, \end{cases} \quad (23)$$

$$r_s = \begin{cases} -\epsilon, & \text{if } s \in \{0, 1, \dots, 8\} \cup \{10, 11, \dots, 18\}, \\ -1 - \epsilon, & \text{if } s = 9, \\ 1 - \epsilon, & \text{if } s = 19, \end{cases} \quad (24)$$

where $U(x)$ is a Heaviside step function defined as

$$U(x) = \begin{cases} 1, & \text{if } x \geq 0, \\ 0, & \text{if } x < 0. \end{cases} \quad (25)$$

\mathbf{G}_v and c_v for $v \in \{0, 1\}$ used in constraint (19d) are

$$\mathbf{G}_0 = \mathbf{E}_{4,4} + \mathbf{E}_{5,5}, \quad (26)$$

$$\mathbf{G}_1 = \mathbf{E}_{6,6} + \mathbf{E}_{7,7}, \quad (27)$$

$$c_0 = c_1 = -1. \quad (28)$$

$\mathbf{J}_{1,u}$ and $\mathbf{p}_{1,u}$ for $u \in \{0, 1, 2\}$ used in constraint (19c) when solving the 1st quadratic programming problem are

$$\mathbf{J}_{1,0} = \mathbf{0}, \quad \mathbf{p}_{1,0} = -\mathbf{e}_3, \quad (29)$$

$$\mathbf{J}_{1,1} = \mathbf{0}, \quad \mathbf{p}_{1,1} = -\mathbf{e}_1 - 4\mathbf{e}_2 + 9\mathbf{e}_3, \quad (30)$$

$$\mathbf{J}_{1,2} = \mathbf{0}, \quad \mathbf{p}_{1,2} = -\mathbf{e}_1 + 4\mathbf{e}_2 + 9\mathbf{e}_3. \quad (31)$$

$\mathbf{J}_{2,u}$ and $\mathbf{p}_{2,u}$ for $u \in \{0, 1, 2, 3\}$ used in constraint (19c) when solving the 2nd quadratic programming problem are

$$\mathbf{J}_{2,0} = \mathbf{0}, \quad \mathbf{p}_{2,0} = \mathbf{e}_3, \quad (32)$$

$$\mathbf{J}_{2,1} = \mathbf{0}, \quad \mathbf{p}_{2,1} = -\mathbf{e}_1 - 4\mathbf{e}_2 + 9\mathbf{e}_3, \quad (33)$$

$$\mathbf{J}_{2,2} = \mathbf{0}, \quad \mathbf{p}_{2,2} = -\mathbf{e}_1 + 4\mathbf{e}_2 + 9\mathbf{e}_3, \quad (34)$$

$$\mathbf{J}_{2,3} = \mathbf{0}, \quad \mathbf{p}_{2,3} = \mathbf{e}_2 - 6\mathbf{e}_3. \quad (35)$$

$\mathbf{J}_{3,u}$ and $\mathbf{p}_{3,u}$ for $u \in \{0, 1, 2, 3\}$ used in constraint (19c) when solving the 3rd quadratic programming problem are

$$\mathbf{J}_{3,0} = \mathbf{0}, \quad \mathbf{p}_{3,0} = \mathbf{e}_3, \quad (36)$$

$$\mathbf{J}_{3,1} = \mathbf{0}, \quad \mathbf{p}_{3,1} = -\mathbf{e}_1 - 4\mathbf{e}_2 + 9\mathbf{e}_3, \quad (37)$$

$$\mathbf{J}_{3,2} = \mathbf{0}, \quad \mathbf{p}_{3,2} = -\mathbf{e}_1 + 4\mathbf{e}_2 + 9\mathbf{e}_3, \quad (38)$$

$$\mathbf{J}_{3,3} = \mathbf{0}, \quad \mathbf{p}_{3,3} = -\mathbf{e}_2 - 6\mathbf{e}_3. \quad (39)$$

$\mathbf{J}_{4,u}$ and $\mathbf{p}_{4,u}$ for $u \in \{0, 1, 2, 3\}$ used in constraint (19c) when solving the 4th quadratic programming problem are

$$\mathbf{J}_{4,0} = \mathbf{0}, \quad \mathbf{p}_{4,0} = \mathbf{e}_3, \quad (40)$$

$$\mathbf{J}_{4,1} = \mathbf{0}, \quad \mathbf{p}_{4,1} = \mathbf{e}_2 + 6\mathbf{e}_3, \quad (41)$$

$$\mathbf{J}_{4,2} = \mathbf{0}, \quad \mathbf{p}_{4,2} = -\mathbf{e}_2 + 6\mathbf{e}_3, \quad (42)$$

$$\mathbf{J}_{4,3} = \mathbf{E}_{2,2} + 9\mathbf{E}_{3,3} + \frac{3}{2}\mathbf{E}_{1,3}, \quad \mathbf{p}_{4,3} = \mathbf{0}. \quad (43)$$

REFERENCES

- [1] Y. Liu, X. Liu, X. Mu, T. Hou, J. Xu, M. Di Renzo, and N. Al-Dhahir, "Reconfigurable intelligent surfaces: Principles and opportunities," *IEEE Communications Surveys & Tutorials*, vol. 23, no. 3, pp. 1546–1577, 2021.
- [2] X. Yuan, Y.-J. A. Zhang, Y. Shi, W. Yan, and H. Liu, "Reconfigurable-intelligent-surface empowered wireless communications: Challenges and opportunities," *IEEE Wireless Communications*, vol. 28, no. 2, pp. 136–143, 2021.
- [3] J. Tang, M. Cui, S. Xu, L. Dai, F. Yang, and M. Li, "Transmissive ris for b5g communications: Design, prototyping, and experimental demonstrations," *IEEE Transactions on Communications*, vol. 71, no. 11, pp. 6605–6615, 2023.
- [4] Y. Liu, X. Mu, J. Xu, R. Schober, Y. Hao, H. V. Poor, and L. Hanzo, "Star: Simultaneous transmission and reflection for 360° coverage by intelligent surfaces," *IEEE Wireless Communications*, vol. 28, no. 6, pp. 102–109, 2021.
- [5] K. W. Cho, M. H. Mazaheri, J. Gummesson, O. Abari, and K. Jamieson, "mmWall: A steerable, transmissive metamaterial surface for NextG mmWave networks," in *20th USENIX Symposium on Networked Systems Design and Implementation (NSDI 23)*. Boston, MA: USENIX Association, Apr. 2023, pp. 1647–1665. [Online]. Available: <https://www.usenix.org/conference/nsdi23/presentation/cho-kun-woo>
- [6] R. Schmidt, "Multiple emitter location and signal parameter estimation," *IEEE Transactions on Antennas and Propagation*, vol. 34, no. 3, pp. 276–280, 1986.
- [7] T. Ma, Y. Xiao, and X. Lei, "Channel reconstruction-aided music algorithms for joint aoa&aod estimation in mimo systems," *IEEE Wireless Communications Letters*, vol. 12, no. 2, pp. 322–326, 2023.
- [8] S. Chen, W. Yang, Y. Xu, Y. Geng, B. Xin, and L. Huang, "Afall: Wi-fi-based device-free fall detection system using spatial angle of arrival," *IEEE Transactions on Mobile Computing*, vol. 22, no. 8, pp. 4471–4484, 2023.
- [9] P. Chen, Z. Yang, Z. Chen, and Z. Guo, "Reconfigurable intelligent surface aided sparse doa estimation method with non-ula," *IEEE Signal Processing Letters*, vol. 28, pp. 2023–2027, 2021.
- [10] Z. Yang, P. Chen, Z. Guo, and D. Ni, "Low-cost beamforming and doa estimation based on one-bit reconfigurable intelligent surface," *IEEE Signal Processing Letters*, vol. 29, pp. 2397–2401, 2022.
- [11] D. Xia, X. Wang, J. Han, H. Xue, G. Liu, Y. Shi, L. Li, and T. J. Cui, "Accurate 2-d doa estimation based on active metasurface with nonuniformly periodic time modulation," *IEEE Transactions on Microwave Theory and Techniques*, vol. 71, no. 8, pp. 3424–3435, 2023.
- [12] M. Abramowitz and I. A. Stegun, *Handbook of mathematical functions with formulas, graphs, and mathematical tables*. US Government printing office, 1968, vol. 55.
- [13] T.-J. Cui, S. Liu, and L.-L. Li, "Information entropy of coding metasurface," *Light: Science & Applications*, vol. 5, no. 11, pp. e16172–e16172, 2016.
- [14] The MathWorks, Inc. Three-dimensional indoor positioning with 802.11az fingerprinting and deep learning. Accessed: 2024-05-07. [Online]. Available: <https://www.mathworks.com/help/wlan/ug/three-dimensional-indoor-positioning-with-802-11az-fingerprinting-and-deep-learning.html>
- [15] Y. Ma, B. Wang, S. Pei, Y. Zhang, S. Zhang, and J. Yu, "An indoor localization method based on aoa and pdoa using virtual stations in multipath and nlos environments for passive uhf rfid," *IEEE Access*, vol. 6, pp. 31772–31782, 2018.
- [16] A. Abdallah and M. M. Mansour, "Efficient angle-domain processing for fdd-based cell-free massive mimo systems," *IEEE Transactions on Communications*, vol. 68, no. 4, pp. 2188–2203, 2020.